J Eng Math (2007) 59:157–169
DOI 10.1007/s10665-007-9142-x

Diffusion fronts in enzyme-catalysed reactions

Graeme P. Boswell · Fordyce A. Davidson

Received: 1 March 2006 / Accepted: 13 February 2007 / Published online: 31 March 2007

Abstract In this paper the nature and validity of the mathematical formulation of Michaelis–Menten-type kinetics for enzyme-catalysed biochemical reactions is studied. Previous work has in the main concentrated on isolated, spatially uniform (well-mixed) reactions. The effects of substrate input and diffusion on this formulation, in particular, on the nature and validity of the *quasi-steady-state-assumption* for diffusion-driven fronts are investigated. It is shown that, provided the Michaelis–Menten constant K_M is sufficiently large, an appropriate quasi-steady-state assumption is valid at all points in space and for all times other than in a region that closely tracks the front itself. Moreover, it is shown that this region shrinks with time.

Keywords Diffusible substrate · Michaelis–Menten · Open system · Quasi-steady state

1 Introduction

One of the fundamental features of enzymatic reactions is enzyme saturation. At saturation of an enzyme, the reaction rate catalysed by the enzyme reaches an apparent maximum, and a further increase of substrate concentration does not appear to enhance the reaction rate. This feature is captured by the Michaelis–Menten formalism [1], which laid the foundation for classical enzyme kinetics. The derivation of this formalism is based on certain assumptions, principally, the *quasi-steady-state assumption* (QSSA) (see e.g. [2,3]). The validity of these assumptions has been the subject of much recent attention. For example, it was initially proposed that a necessary condition for the standard or classical assumption (sQSSA) is that the initial substrate concentration greatly exceeds that of the enzyme. This situation often arises in laboratory experiments, but is less common for reactions in vivo. Consequently, new, weaker necessary conditions on the initial concentrations have subsequently been derived (see e.g. [3]).

G. P. Boswell
Division of Mathematics and Statistics, Faculty of Advanced Technology, University of Glamorgan, Pontypridd, Wales CF37 1DL, UK

F. A. Davidson (✉)
Department of Mathematics, University of Dundee,
Dundee DD1 4HN, Scotland, UK
e-mail: fdavidso@maths.dundee.ac.uk

Almost all previous work has concentrated on reactions with no substrate input. Therefore, strictly speaking, the conclusions drawn are only valid for isolated enzymatic reactions. In a living system, large numbers of enzymatic reactions are networked in a complex manner. Pathways can be unidirectional, reversible, branched, or cyclic [4]. A particular enzymatic reaction is embedded in such a pathway, taking product molecules from the previous reaction step and supplying substrate to the next step. Moreover, a living system may take up substrates from external sources and release products to them. Therefore, all enzymatic reactions in a living system are subject to substrate input and product removal. In order to understand the function of biochemical reactions in vivo using enzyme kinetics, it is therefore essential to determine the validity of this approach under such conditions. Some progress has been made in this direction, see e.g. [5–7]. In [8,9], as a reasonable and biologically relevant first step, the effects of a constant substrate input on the derivation and validity of classical quasi-steady-state assumptions were investigated. Necessary conditions for the validity of these assumptions were derived and were shown to be dependent on the input I. Also, it was discovered that, even in the case where the introduction of (a possible sufficiently large) input maintains or widens the applicability of a QSSA, the time scales associated with the transient and QSS periods, the form of the quasi-steady-state solution itself, and the associated reaction-rate equation are all dependent on I. Therefore, the formalism established in the absence of input *does not*, in general, provide accurate information regarding systems with input. In [10], this work was extended to consider periodic inputs.

In [11], Maini et al. extended the no-input enzyme-catalysed system to allow for the biologically relevant case in which the substrate diffuses while the enzyme remains essentially fixed (in a cell membrane for example — see also [12]). It is this work that will form the main focus here.

In Sect. 2, a model system for an enzyme-catalysed reaction that is subject to a constant non-negative substrate input is introduced. The QSSA for this problem is then studied in Sect. 3 where certain validity conditions are discussed, and this work is extended in Sect. 4 where the effect of a point source of input is investigated. Finally, in Sect. 5, we conclude with a short discussion.

2 Enzyme–substrate reactions with input

The reaction we shall discuss can be represented schematically as shown in Fig. 1.

Here, I denotes substrate input, and E, S, C, and P denote, respectively, the free enzyme, free-substrate, enzyme–substrate complex and the product. The spatio–temporal evolution of the concentrations of the reactants can be described by the following system of partial differential equations:

$$\frac{\partial E}{\partial t} = -k_1 ES + k_{-1} C + k_2 C, \tag{1a}$$

$$\frac{\partial S}{\partial t} = I - k_1 ES + k_{-1} C + D\nabla^2 S, \tag{1b}$$

$$\frac{\partial C}{\partial t} = k_1 ES - k_{-1} C - k_2 C, \tag{1c}$$

together with the decoupled equation for the product production rate,

$$\frac{\partial P}{\partial t} = k_2 C. \tag{1d}$$

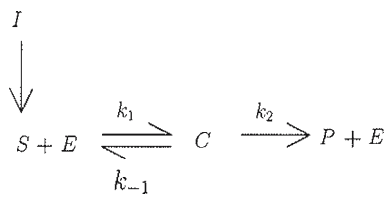

Fig. 1 The enzyme–substrate reaction with substrate input

(For notational convenience we have denoted the concentrations of each of the reactants by the corresponding letter and substrate input is denoted by I.) The diffusion of the substrate is modelled using Fickian diffusion with coefficient D and it is assumed that this process does not alter the reaction rates (see [12]). These equations are assumed to hold in some spatial domain, Ω, which we will assume to be unbounded. Physically, this represents a large domain within which the reaction takes place without interaction with the boundary. To complete the mathematical formulation, this system is augmented with initial data of the form

$$E(\boldsymbol{r},0) = E_0, \quad S(\boldsymbol{r},0) = S_0(\boldsymbol{r}), \quad C(\boldsymbol{r},0) = P(\boldsymbol{r},0) = 0, \tag{2}$$

where $\boldsymbol{r} \in \Omega$ is the spatial variable, E_0 is a constant and $S_0(\boldsymbol{r})$ is some prescribed function of $\boldsymbol{r}$. We seek solutions that decay sufficiently fast as $|\boldsymbol{r}| \to \infty$.

By adding (1a) and (1c), it follows from (2) that

$$\frac{\partial (E + C)}{\partial t} = 0 \implies E(\boldsymbol{r},t) + C(\boldsymbol{r},t) \equiv E_0.$$

Hence, the original system (1a–1c) reduces to

$$\frac{\partial S}{\partial t} = I(\boldsymbol{r},t) - k_1(E_0 - C)S + k_{-1}C + D\nabla^2 S, \tag{3a}$$

$$\frac{\partial C}{\partial t} = k_1(E_0 - C)S - k_1 K_M C, \tag{3b}$$

for $\boldsymbol{r} \in \Omega$, $t > 0$ with

$$C(\boldsymbol{r},0) = 0, \quad S(\boldsymbol{r},0) = S_0(\boldsymbol{r}). \tag{4}$$

The composite parameter $K_M := (k_{-1} + k_2)/k_1$ is called the Michaelis–Menten rate constant.

This system is similar to that investigated by Merkin and Sleeman [13] where the interaction of a free morphogen with a fixed ligand receptor is studied. Letting S and C denote the concentration of morphogen and receptor, respectively, the system studied in [13] is given by (3) with $I \equiv 0$. The spatial domain is assumed to be one dimensional and the input of morphogen is represented by a non-zero Dirichlet condition for S at the spatial origin. A nondimensionalisation is carried out to allow an analysis of the system for various asymptotic limits of the parameters. In particular, an in-depth analysis of wave-front solutions (similar to those shown below) is made in the case where $k_{-1} = 0$ and for $k_{-1} > 0$, a considerable understanding of the solutions structure is obtained in the special cases where k_2/k_{-1} is large and the input of morphogen is large. However, we will not pursue this line of analysis in this paper because we are principally interested in the direct spatial extension of the system studied in [9,10] and the system studied by Maini et al. in [11]. As such we are interested in obtaining a better understanding of the dynamics of system (3) via the *quasi-steady-state assumption*.

The quasi-steady-state assumption (QSSA) is that the complexes react very rapidly with free-substrate and therefore the concentration is in a "steady-state" with respect to the substrate concentration, i.e., for any given value of S, $\frac{\partial C}{\partial t} = 0$. Thus, system (3) reduces to the differential-algebraic system

$$\frac{\partial S}{\partial t} = I(\boldsymbol{r},t) - \frac{k_2 E_0 S}{S + K_M} + D\nabla^2 S, \tag{5a}$$

$$C = \frac{E_0 S}{S + K_M}. \tag{5b}$$

This system is the quasi-steady state approximation for (3). In the following, we will consider how the validity of this approximation depends on the reaction parameters, in particular on the value of the Michaelis–Menten rate constant K_M. The focus of laboratory experiments regarding biochemical reaction rates is often to determine this rate constant. In many situations this constant can be very large relative to other reaction parameters (see [4]).

2.1 Special cases

For $D = 0$ and $I \equiv 0$, system (3) becomes the classic, spatially uniform, closed, Michaelis–Menten system, which has received extensive attention. In this case, a necessary condition for the validity of the classic or standard quasi-steady-state assumption (sQSSA) is

$$E_0 \ll S_0 + K_M. \tag{6}$$

If this condition is satisfied, system (3) undergoes a rapid transient in which the substrate concentration is almost unaltered and then the dynamics of the system closely follow those of the reduced system (5) augmented with the initial data $S(0) = S_0$. Appropriate time scales for the transient and QSS phases are, respectively,

$$t_{tr} = \frac{1}{k_1(S_0 + K_M)} \quad \text{and} \quad t_q = \frac{S_0 + K_M}{k_2 E_0}.$$

Here, t_{tr} is the relaxation time of the transient period and t_q gives a scaling for the length of time it takes the system to return to the steady state ($S = C = 0$) during the QSS phase. The necessary condition ensures that $S \approx S_0$ during the transient and that $t_{tr} \ll t_q$.

With $D = 0$ and $I = I_0 > 0$, system (3) reduces to the spatially uniform, but open system studied in [9]. The time scales detailed above are modified accordingly and, as it is shown in [9], the necessary condition for the validity of the sQSSA is

$$E_0 \ll S_0 + \hat{S} + K_M,$$

where $(\hat{S}, \hat{C}) = (K_M I_0/k_2 E_0, I_0/k_2)$ is the corresponding positive, uniform steady state of (3). It follows that increasing the input I_0 increases the range of other system parameters and initial data for which the sQSSA holds.

For $D = 0, I = I(t)$ estimates for the times scales and validity condition can be made in the case where $I(t)$ is periodic with positive mean value I_0 [see 10].

For $I \equiv 0$ but $D > 0$, Maini et al. [11] considered system (3) with $\Omega = \mathbf{R}^2$ and $S(\boldsymbol{r}, 0) = S_0 \delta_2(\boldsymbol{r})$ where $\delta_2(\boldsymbol{r})$ denotes the Dirac delta function for $\mathbf{R}^2$. In this case, radially symmetric solutions exist. It was shown through numerical integration that for parameter values suitably chosen, the solutions of the full system (3) and those of the reduced system (5) were in close agreement initially inside an expanding annulus. This annulus decreases in width with increasing time. Thus, after sufficient time, an expanding disk forms in the plane inside which it is concluded the QSSA does not hold, the fall in substrate concentration in the wake of the reaction–diffusion front is given as the reason.

3 Diffusing substrate with no input

We begin by reconsidering the no-input case studied in [11], i.e., Eqs. (3) with $I \equiv 0$ but $D > 0$. In this case the associated quasi-steady-state equations are given by (5) with $I \equiv 0$. Radially symmetric initial data (4) ensures that solutions of (3) and (5) are radially symmetric and henceforth we shall only consider such solutions, which therefore only depend on the distance r from the origin in $\mathbf{R}^2$.

To avoid ambiguity, we will use the variables S and C to denote the free-substrate and enzyme–substrate complex concentrations of the full system described in Eq. (3) and the variables S_q and C_q to denote the corresponding variables in the QSS system (5).

3.1 Numerical solution

Our main aim is to ascertain under what conditions the dynamics of system (5) provide a good approximation to those of the full system (3). To this end, system (3) with initial data (4) was solved numerically

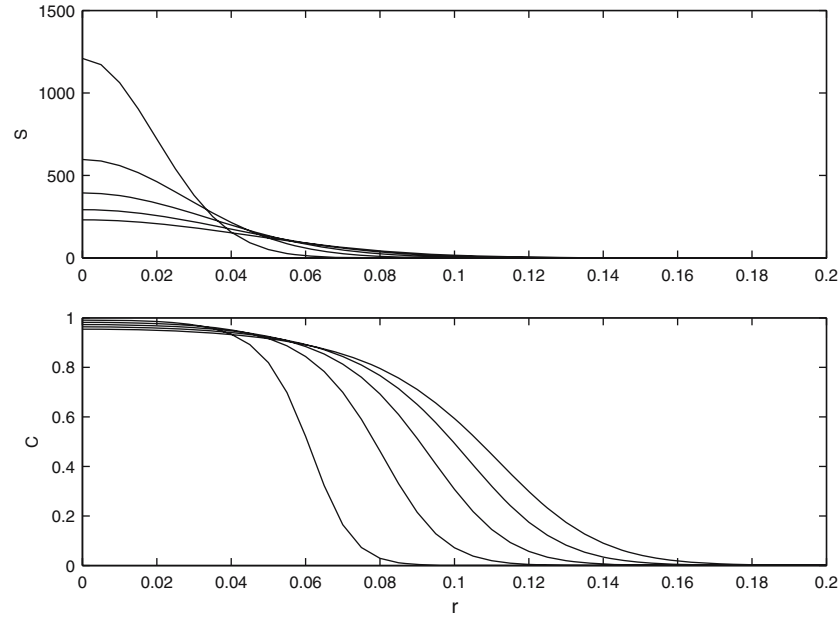

Fig. 2 The distributions of the free substrate S and enzyme–substrate complex C obtained by numerically integrating the full system given in Eq. (3) with initial data (4) (with the delta function being approximated by a tent function) are shown at times $t = 2, 4, 6, 8, 10$. Other parameters are $D = 10^{-4}, K_M = 11, (k_1 = 1, k_2 = 1, k_{-1} = 10), E_0 = 1, S_0 = 3, I \equiv 0$. Numerically obtained solutions of the reduced system (5) are graphically indistinguishable from those obtained by solving the full system (3)

for $0 \leq r \leq 1$ using finite differences (see [14]). (In all the results described below, the numerical solution was stopped before the leading edge of substrate could interact with the boundary.) Parameter values were chosen such that in the absence of diffusion, the sQSSA would be valid. In [11], it was discussed that for many realistic biochemical reactions, the reaction parameter K_M is often large. Therefore, we pay particular attention to how properties of the system and its approximation vary with K_M.

As illustrated in Fig. 2, the substrate S diffuses from the origin and reacts with the enzyme to produce the enzyme–substrate complex. The resultant complex distribution propagates outwards from the origin in a wave-like manner, exhibiting only a small and slow decrease in the complex concentration behind the wavefront. The QSSA equations (5) were solved similarly, and the corresponding values of S_q and C_q proved to be qualitatively and quantitatively very similar to S and C obtained from the full system. However, it was observed that $S \leq S_q$ and $C \leq C_q$ for all $r \in [0, 1]$ throughout the duration of the integration process (see also later).

3.2 Position of the front

The spread of the substrate from the origin can be quantitatively measured by determining the position of its leading edge r_α, which is the value of r where the substrate takes a given value α, i.e., $\alpha = S(r_\alpha, t)$ [see also ref. 13]. The initial substrate is located at the origin and therefore the initial value of r_α is zero. As the substrate diffuses from the origin, the value of r_α initially increases (Fig. 3). However, due to the enzyme reaction, the substrate is steadily depleted, causing the value of r_α to decrease back towards zero. The rate at which the substrate edge expands from and retracts back to the origin increases with increasing values of the parameter K_M (Fig. 3).

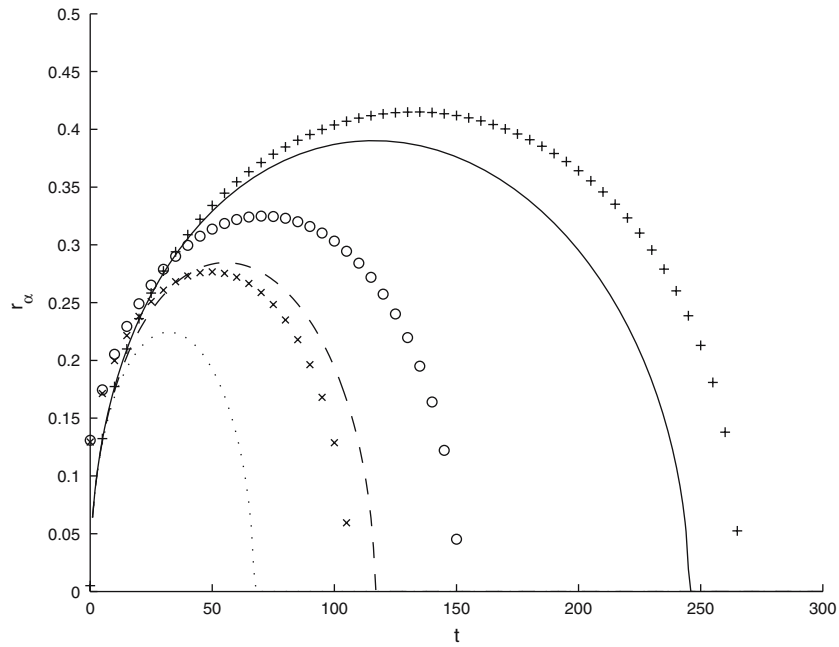

Fig. 3 The value r_α such that $\alpha = S_q(r_\alpha, t)$ is determined by solving Eq. (5) with initial data (4) with $\alpha = 1/4\pi$ for differing values of K_M and compared to analytical approximations obtained from (16) with $k = k_2 E_0/K_M$, representing a lower bound on the position of the substrate edge. The data points $\times$, $\circ$ and $+$ denote the position of the leading substrate edge determined by numerically solving the full system of equations with K_M taking values 11, 21 and 51, respectively. The corresponding analytical approximations (dotted, dashed and solid lines) obtained from Eq. 16 are shown. The remaining parameter values are $k_2 = 1, S_0 = 3, E_0 = 1, D = 10^{-4}$

3.3 Error in using the reduced system

In [11], an error function is used to compare the substrate concentration obtained from solving the full system (3) to that obtained from solving the QSS system (5) in an attempt to delineate regions of $\mathbf{R}^2$ where the QSSA is and is not valid. In our notation, this error function is given by $E_M := 2(S_q - S)/(S_q + S)$, that is, the difference between the substrate concentrations expressed as a proportion of their average, and, since $S_q \geq S \geq 0$, takes values between 0 and 2. For the simulations described above, this error is small behind the advancing substrate front and rises to its maximum value at the leading edge. However, this error only makes physical sense when there is a "non-negligible" amount of substrate to measure. Thus, we consider the error E_M only where the substrate concentration exceeds some prescribed minimum value (10^{-6} was used throughout).

The error E_M thus determines a narrow region in $r - t$ space that closely tracks the position of the advancing substrate front (Fig. 4). This region expands, then contracts over time, and eventually disappears, since the region in which there is a non-negligible amount of substrate initially expands from and then retracts back to the origin while the region in which the error E_M is considered large continues to expand from the origin. The maximum width of this region decreases with increasing values of K_M. Within this region, it can be viewed that the reduced system (5) does not provide a good approximation to the full system (3).

3.4 Further analysis of front propagation and the QSSA

In order to investigate further some of the properties highlighted by the numerical simulations discussed above, we first consider a class of related, linear equations. Consider the equation

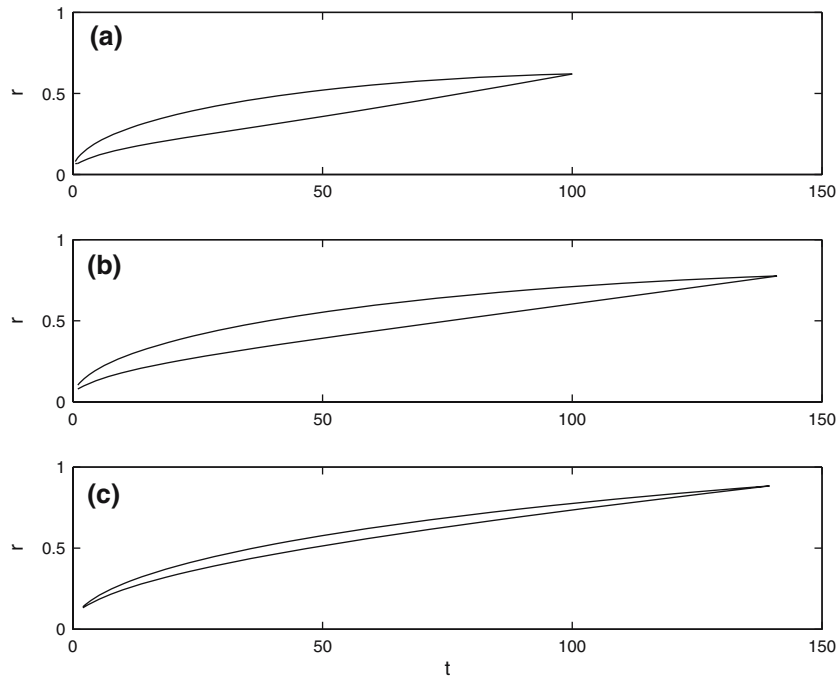

Fig. 4 The region in $r-t$-space inside which the error $E_M := 2(S_q - S)/(S_q + S) > 0.2$ and the substrate concentration $S > 10^{-6}$. The inner and outer bounds of this region, corresponding to the position where $E_M = 0.2$ and $S = 10^{-6}$, respectively, are plotted over time for parameter values $k_1 = 1, k_2 = 1, S_0 = 3, E_0 = 1, D = 10^{-4}$ with (**a**) $K_M = 11 (k_1 = 10)$, (**b**) $K_M = 21 (k_1 = 20)$, and (**c**) $K_M = 51 (k_1 = 50)$

$$\frac{\partial u}{\partial t} = -ku + D\nabla^2 u, \quad r \geq 0, \quad t > 0, \tag{7}$$

with initial data $u(r, 0) = S_0 \delta(r)/2\pi r$, where $\delta(r)$ denotes the standard Dirac delta function. It is well-known that this equation has a unique, positive solution, which we denote by $u(k, r, t)$, and which has closed form [see, e.g. ref. 15]

$$u(k, r, t) := \frac{S_0}{4\pi Dt} \exp\left(-kt - \frac{r^2}{4Dt}\right). \tag{8}$$

It is straightforward to show that $u(0, r, t)$ and $u(k_2 E_0/K_M, r, t)$ are, respectively, upper and lower solutions for (5a). Hence a unique solution, S_q, of (5a) exists and

$$u(k_2 E_0/K_M, r, t) \leq S_q(r, t) \leq u(0, r, t), \quad r \geq 0 \quad \text{and} \quad t > 0, \tag{9}$$

(see for example, [16, Chapter 7]). This unique solution generates an unique description of $C_q(r, t)$ given by (5b). It follows directly that $u(k_2 E_0/K_M, r, t)$ becomes an increasingly accurate approximation for S_q as K_M is increased.

By similar techniques it can be shown that the full system (3) admits solutions that are positive for all $t > 0$ and that $0 < C(r, t) \leq C_q(r, t)$. Moreover, given any such positive solution (S, C), it can be shown that

$$u((k_{-1} + k_2)E_0/K_M, r, t) \leq S(r, t) \leq S_q(r, t), \quad r \geq 0, \quad t > 0. \tag{10}$$

These bounds underpin the numerical simulations detailed above.

In the limit as $K_M \to \infty$, it is straightforward to show that $u((k_{-1}+k_2)E_0/K_M, r, t) \to u(0, r, t)$ pointwise in r and t for all $(r, t) \in \{r \geq 0, t > 0\} \bigcup \{r > 0, t \geq 0\}$ and uniformly for all $(r, t) \in \{r \geq 0, t \geq t_0\} \bigcup \{r \geq r_0, t \geq 0\}$ for any t_0, $r_0 > 0$. Hence $S(r, t) \to S_q(r, t)$ pointwise, respectively uniformly, in r and t in the same regions.

It appears from the above estimates that the QSSA for the spatially extended case should hold (in some sense) for K_M sufficiently large. The necessary conditions for the validity of the QSSA in the classic, spatially uniform case are, as noted above, that the substrate concentration remains unaltered during the transient and that the transient time scale is much smaller than that for the QSS phase.

First consider the transient phase in the spatially extended case. During this phase, suppose that it is assumed that complexes react quickly with any available substrate, leaving the concentration of the latter essentially unaltered. For the spatially extended case, at $t = 0$, $S = 0$ at all points except $r = 0$. For $t > 0$ the substrate concentration progresses out in a diffusion-driven front. The complexes initially react at this front, ahead of which the substrate concentration is effectively zero. Therefore, at any fixed point in space, the substrate concentration is initially zero and then rises before falling again as the wave front passes. So, the complexes initially react with an increasing concentration of substrate. However, if we assume that the complexes react sufficiently quickly with any substrate available, then from (3b) with $S \equiv \hat{S}(r)$, it can be deduced that the half life of the transient phase is,

$$t_h = \frac{1}{k_1(K_M + \hat{S}(r))},$$

for whatever substrate concentration $\hat{S}(r)$ is available at that given point r. It follows that t_h is small uniformly in r if K_M is sufficiently large. Hence, we propose that a (conservative, over-) estimate for the transient time scale is

$$t_{tr} := \frac{1}{k_1 K_M}.$$

In order to check the validity of this assumption, we must determine whether the substrate concentration really does remain unaltered during this transient period. It appears very difficult to establish this result at each point in space. However, it is possible to consider how the total mass of substrate changes over the given time period as follows. The initial mass of substrate in the system is S_0. Integrating both sides of (3a) over $\mathbf{R}^2$ and on noting the boundary conditions at $r = 0$ and $r = \infty$, yields

$$m'(t) := \frac{\mathrm{d}}{\mathrm{d}t}\int_0^\infty S(r,t)2\pi r \mathrm{d}r = \int_0^\infty \left[-k_1(E_0 - C(r,t))S(r,t) + k_{-1}C(r,t)\right]2\pi r \mathrm{d}r. \tag{11}$$

Following [3], we define the relative change in mass over the transient period as

$$\left|\frac{\Delta m}{S_0}\right| \approx t_{\mathrm{tr}}\frac{1}{S_0}\left|m'(t)\right|_{\max}, \tag{12}$$

where the maximum of m' is taken over the transient period. On noting that $C(r,0) = 0$ and $|m'|$ is decreasing in the first instance, it follows from (11) and (12) that

$$\left|\frac{\Delta m}{S_0}\right| \approx \frac{E_0}{K_M S_0}. \tag{13}$$

Hence, demanding that this relative change is small requires

$$E_0 \ll K_M S_0. \tag{14}$$

Let us now consider the QSS period. Recall that, in this period, it is supposed that the dynamics of the full system (3) are governed by (5). Hence, on integrating (5a) over $\mathbf{R}^2$ and again recalling the boundary conditions, we have that

$$m_q'(t) := \frac{\mathrm{d}}{\mathrm{d}t}\int_0^\infty S_q(r,t)2\pi r \mathrm{d}r = \int_0^\infty \frac{-k_2 E_0 S_q(r,t)}{K_M + S_q(r,t)}2\pi r \mathrm{d}r. \tag{15}$$

Again following [3], we can estimate the time scale of the QSS period by

$$\frac{|m_{q_{\max}} - m_{q_{\min}}|}{\left|m_q'(t)\right|_{\max}} \geq \frac{K_M}{k_2 E_0},$$

as $\left|m_q'(t)\right|_{\max} \leq k_2 E_0 S_0 / K_M$. If we define $t_q := K_M/k_2 E_0$, then t_q provides an (under) estimate for the QSS time scale of the total mass.

The above time scale again takes no account of spatial variation and this we now do. Again considering the linear equation (7), it is straightforward to show that the position, r_α, at which the solution (8) attains a value, α, say, for some positive number α, is given by the equation

$$r_\alpha(t) = 2\sqrt{Dt}\left[-kt + \log\left(\frac{S_0}{4Dt\pi\alpha}\right)\right]^{1/2}, \tag{16}$$

which holds provided $0 < t \leq t^*$ where t^* is the unique positive solution of $kt = \log\left(\frac{S_0}{4Dt\pi\alpha}\right)$. It follows that

$$t^* \leq \frac{S_0}{4D\pi\alpha} =: t_d, \quad \text{and} \quad \lim_{k\to 0} t^* = t_d.$$

The time t^* gives a measure of the time taken for the solution to "level out" and depends both on the reaction kinetics and the diffusion rate. During this time period, the substrate concentration at each point in space is changing due to the passing and relaxation of the diffusive wave. The diffusive time scale can be isolated as t_d. From (9), (10) and the above arguments, in the case K_M is sufficiently large, this time scale also provides a good estimate for the corresponding time scale for system (5) and thus (3). It seems reasonable then, to demand that this time scale is also large compared to the transient time scale.

We therefore have the following proposition.

Proposition 1 *Necessary conditions for the validity of the quasi-steady-state assumption in the spatially extended case with no input are:*

1. *the change in total mass of substrate during the transient period must be small;*
2. *the transient time scale must be much less than the total-mass QSS time scale;*
3. *the transient time scale must be much less than the diffusion time.*

From the above we see that these conditions are certainly satisfied if

$$E_0 \ll K_M S_0, \quad k_2 E_0 \ll k_1 K_M^2 \quad \text{and} \quad D \ll k_1 K_M S_0,$$

where in the last inequality we have taken $\alpha = 1/4\pi$ without loss of generality. In fact, the first inequality is stronger than the second and so the conditions reduce to

$$E_0 \ll K_M S_0 \quad \text{and} \quad D \ll k_1 K_M S_0. \tag{17}$$

Both of these inequalities are satisfied if either S_0 or K_M is sufficiently large. The second inequality suggests that, if the QSSA is valid for $D = 0$ (for example K_M is fixed and sufficiently large), these necessary conditions continue to hold provided D is sufficiently small.

4 Substrate input

In [9,10] constant and periodic, spatially uniform inputs are considered, respectively. Here we shall consider an input of constant magnitude, which is localised at the origin. Hence, we shall now consider

$$I(\boldsymbol{r}, t) = I(r) := \frac{I_0}{2\pi r}\delta(r),$$

i.e., a point source at $r = 0$ with total input per unit time equal to some positive constant I_0.

First, notice that, in this case, system (3) has a non-trivial steady state which is given by the corresponding steady state of system (5). Hence, Eq. (5) always provides a "good approximation" to the solutions of the full system, provided t is sufficiently large. (This is also the case above where the only steady state is the trivial one.) For an analysis of the dynamics over a shorter time scale we must proceed as above.

4.1 Numerical solutions

The equations of (3) of the full system were solved numerically using the initial data and boundary conditions as previously described. The expansion of the distribution slows over time and tends towards a steady state, the shape of which is determined by the input rate I_0 and the value of K_M (see Figs. 5, 6).

The equations of the reduced system (5) were solved in a similar manner, with the distributions of S_q and C_q displaying the same behaviour as the full system. Again it was observed that $S(r,t) \leq S_q(r,t)$ and $C(r,t) \leq C_q(r,t)$ for all $r, t \geq 0$.

The solution of the full system (3) and that obtained through applying the QSSA, i.e., Eqs. 5 can be compared via the error E_M defined above. By investigating the numerical solutions over a range of parameter values, it appears that the QSSA is valid in all regions of space and for all times other than in an annular region that closely tracks the reaction front (Fig. 7). The time interval over which this annulus exists increases with the input rate I_0 and the maximum width of the annulus decreases as K_M increases.

4.2 Bounds on the front position and conditions for the QSSA

If we add $I(r)$ to the right-hand side of (7), then the solution is now given by (see again [15])

$$u_I(k,r,t) := \frac{S_0}{4\pi Dt} \exp\left(-kt - \frac{r^2}{4Dt}\right) + \int_0^t \frac{I_0}{4\pi D(t-\tau)} \exp\left(-k\tau - \frac{r^2}{4D\tau}\right) \mathrm{d}\tau. \tag{18}$$

With this new definition, using similar arguments to those above, we can show that bounds corresponding to (9) and (10) still hold. Moreover, it follows that in the limit as $K_M \to \infty$, the solutions of the full system tend to those of (5), uniformly in r and t for $(r,t) \in \{(r,t) \,|\, r \geq r_0, t \geq t_0\}$ for any $r_0, t_0 > 0$. Moreover, for K_M sufficiently large, $u_I(k_2 E_0/K_M, r, t)$ is a good approximation for $S_q(r,t)$ and thus for $S(r,t)$.

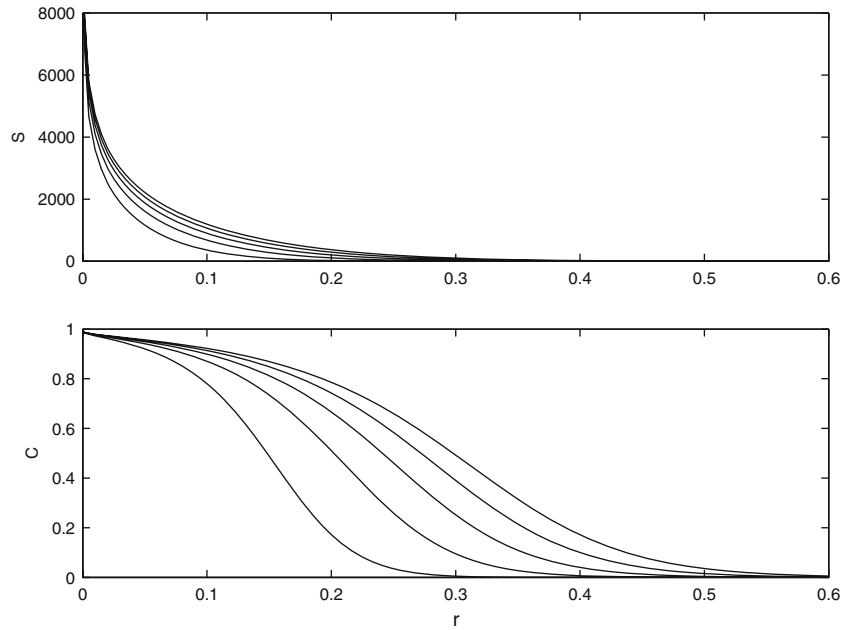

Fig. 5 The distributions of the free substrate S and enzyme–substrate complex C obtained by numerically integrating the full system given in Eq. 3 with initial data (4) (with the delta function being approximated by a tent function) are shown at times $t = 40, 80, 120, 160, 200$. Other parameters are $D = 10^{-4}, k_1 = 1, k_2 = 1, k_{-1} = 100, (K_M = 101), E_0 = 1, S_0 = 3, I_0 = 1$

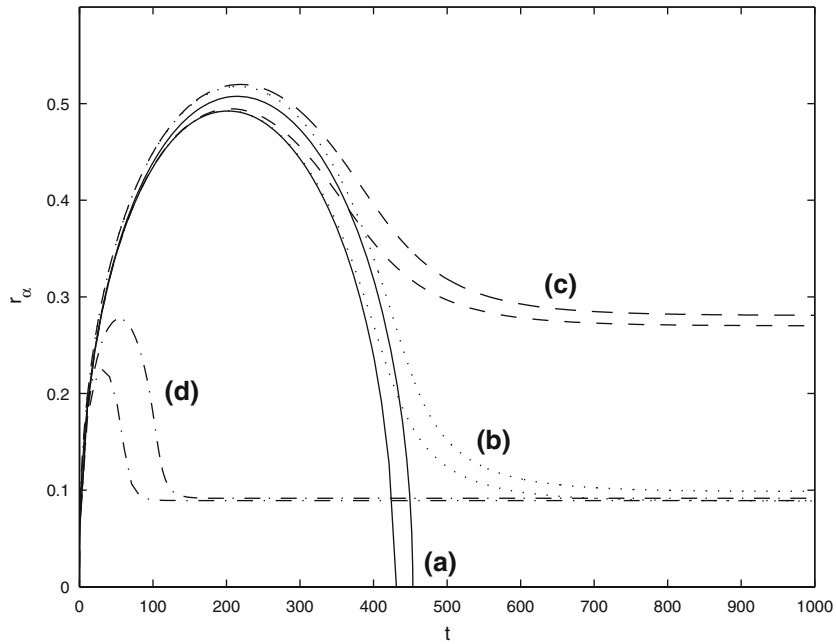

Fig. 6 The value of r_α for which $\alpha = u_I(k_2E_0/K_M, r_\alpha, t)$ where u_I is defined in Eq. 18 is compared to that obtained by numerically solving the full system (3) for different input rates I_0. The position of the leading edge obtained by solving the reduced system (5) is graphically indistinguishable from that obtained by the solving the full system. The leading edge value α is taken to be $\frac{1}{4\pi}$ and the remaining parameter values are $D = 10^{-4}, k_1 = 1, k_2 = 1, E_0 = 1, S_0 = 3$ with (**a**) $I_0 = 0, K_M = 101$, (**b**) $I_0 = 10^{-4}, K_M = 101$, (**c**) $I_0 = 10^{-3}, K_M = 101$ and (**d**) $I_0 = 10^{-3}, K_M = 11$. In each case, the higher curve denotes the position of the leading edge obtained through numerical integration of (3) and the lower curve denotes the lower bound obtained by solving Eq. 18

On assuming $S \equiv \hat{S}$ in (3b), the transient time scale can be computed as above and shown to be $t_{tr} = 1/k_1K_M$ and hence independent of the input I. Demanding that the relative change of total mass is small during the transient period now requires

$$|I_0 - k_1E_0S_0| \ll k_1K_MS_0. \tag{19}$$

One can check that this bound is intuitively correct, in that for large inputs of substrate, the total mass would be changing (increasing) rapidly and hence it could not be expected that the substrate concentration all points remains unaltered during a (fixed) time period of order t_{tr}.

It is difficult to gain any quantitative information regarding how the input affects the QSS time scale. However, upon setting $k = k_2E_0/K_M$, tracking the point r_α for which $\alpha = u_I(r_\alpha, t)$, shows that the solutions reach a steady state for all inputs (Fig. 6). This corresponds to a lower bound for the position of the leading substrate edge. Indeed, the maximum relative difference between the position r_α determined by solving (18) and the full model equations decreases with increasing K_M (see Fig. 6), while the final (steady-state) position of the substrate edge as determined by Eq. 18 is in very good agreement with that computed via the full system (3).

5 Discussion

The well-known standard quasi-steady-state assumption (QSSA) was originally formulated to consider reactions in homogeneously mixed conditions that are closed to any external factors. However, when either the closure or the homogeneity of the system is relaxed, it is unclear under what conditions the corresponding "QSSA" is valid. Such considerations are essential for realistic applications in which a given

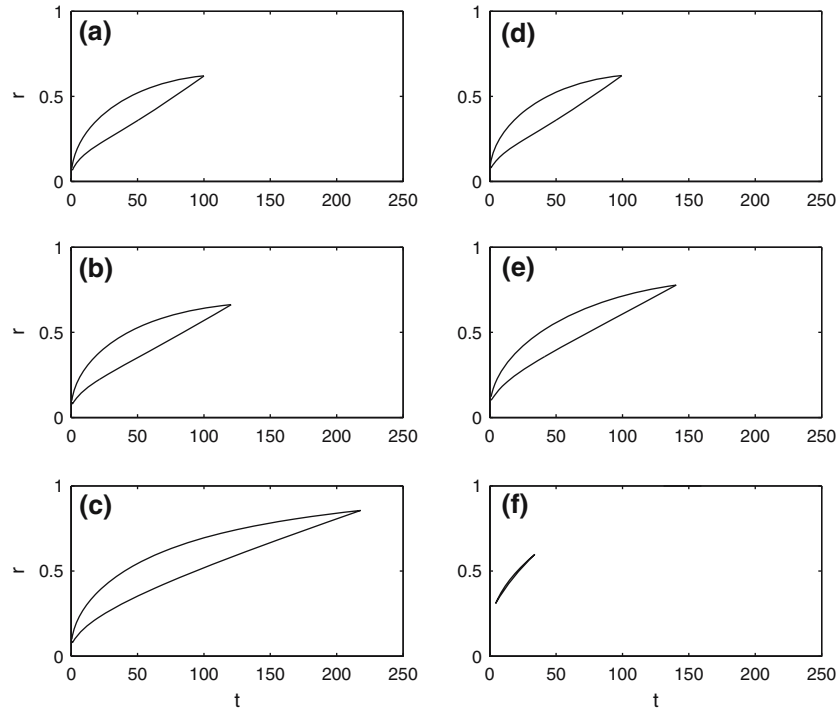

Fig. 7 Equations 3 and 5 are solved numerically giving rise to an annular region expanding from the origin inside which the error $E_M = 2(S_q - S)/(S_q + S) > 0.2$ and the substrate concentration $S > 10^{-6}$. The inner and outer boundaries, corresponding to the position where $E_M = 0.2$ and $S = 10^{-6}$, respectively, are plotted over time for parameter values $k_1 = 1, k_2 = 1, S_0 = 3, E_0 = 1, D = 10^{-4}$ with (**a**) $I_0 = 0, K_M = 11$, (**b**) $I_0 = 0.1, K_M = 11$, (**c**) $I_0 = 1, K_M = 11$, (**d**) $I_0 = 10^{-3}, K_M = 11$, (**e**) $I_0 = 10^{-3}, K_M = 21$, and (**f**) $I_0 = 10^{-3}, K_M = 101$

biochemical reaction is very often imbedded in a chain of reactions. Moreover, it cannot always be assumed that the reactants are free to mix in a homogeneous manner; reactions on cell membranes are a typical example of where the enzyme may be essentially fixed and exposed to a diffusing substrate.

In this paper, it has been shown that in a simple, spatially extended enzyme–substrate "Michaelis–Menten" reaction, a front of enzyme–substrate complex formation and subsequent product generation is driven by the diffusing substrate concentration. In the absence of substrate input, this reaction is eventually exhausted. However, with substrate input (restricted to the origin), a non-trivial steady state is reached and complex formation and product generation is sustained indefinitely. In this work we have shown that both input and spatial movement (diffusion) of substrate, significantly affects the conditions under which a usable QSSA can be applied to understand these dynamics. In particular, in the case of no substrate input but substrate diffusion, we propose that the well-established validity condition (6) is replaced by the inequalities (17). The latter condition is certainly satisfied if the Michaelis–Menten constant K_M is sufficiently large. It appears that K_M sufficiently large is also a sufficient condition for the validity of the QSSA when substrate input is included. Moreover, when K_M is sufficiently large, it has been shown here that certain important quantitative and qualitative features of the full reaction system (3) are in fact approximated well by the solutions of the linear equation (7). As would be expected, the QSSA does not hold uniformly in space at all times: the region around the reaction front is where the greatest error in applying this approximations occurs. This region is narrowed by increasing K_M.

As pointed out in the discussions above, the asymptotic (steady) states of the full system (3) and the approximate system (5) are the same. Hence, close to the steady state (e.g. for large times), it is clear that

the latter provides a good approximation to the former, uniformly in space. Furthermore, for intermediate times, it is clear from (9) and (10) that the solutions of (5) must provide a good approximation to those of system (3) under certain circumstances. Lastly, our error calculations support these estimates showing that the relative difference between solutions of the full system and those of the approximate system can be made small (for sufficiently large K_M) in all regions in space, apart from in an area that closely tracks the reaction front and which only lasts for a finite time. These results seem to be at odds with the conclusions drawn in [11], perhaps suggesting that either the parameter values used in [11] are not in the correct range for the applicability of the QSSA or that there is some ambiguity in the interpretation of the data presented there. Certainly the explanation given of why the QSSA does not hold behind the expanding reaction front does not seem sufficient: the reason given is that, after the passing of the reaction-wave front, the substrate concentration then reduces as it is converted to complexes and thence to products. However, this is exactly what happens during the QSS phase of the classic, spatially uniform case.

Traditionally, conditions on the initial values of the substrate and enzyme concentrations have been used to establish the validity of the QSS approximation. However, although these are measurable and controllable for reactions in vitro, the concept of "initial data" for reactions in vivo is less clear. Therefore, the dependence of the applicability of the QSSA on the rate constant K_M derived above is important with regards to its application, as it is often the case this rate constant is either known or measurable for a given biochemical reaction.

References

1. Michaelis L, Menten ML (1913) Die kinetik der invertinwirkung. Biochem Z 49:333–369
2. Segel LA (1988) On the validity of the steady state assumption of enzyme kinetics. Bull Math Biol 50:579–593
3. Segel LA, Slemrod M (1989) The quasi-steady-state assumption: a case study in perturbation. SIAM Review 31:446–477
4. Stryer L (1995) Biochemistry. W. H. Freeman and Company, New York
5. Battelli F, Lazzari C (1986) Singular perturbation theory for open enzyme reaction networks. IMA J Math Appl Med Biol 3(1):41–51
6. Palson BO, Lightfoot EN (1984) Mathematical modelling of dynamics and control in metabolic networks. I. On Michaelis–Menten kinetics. J Theor Biol 111(2):273–302
7. Schauer M, Heinrich R (1979) Analysis of quasi-steady-sate approximation for an enzymatic one-substrate reaction. J Theor Biol 79:425–442
8. Stoleriu I, Davidson FA, Liu JL (2002) Asymptotic approximations for Michaelis–Menten type kinetics for enzyme-catalysed reactions with constant input. Applied Analysis Report 021, University of Dundee
9. Stoleriu I, Davidson FA, Liu JL (2004) Quasi-steady state assumptions for non-isolated enzyme-catalyzed reactions. J Math Biol 48:82–104
10. Stoleriu I, Davidson FA, Liu JL (2005) Effects of periodic input on the quasi-steady state assumptions for enzyme-catalysed reactions. J Math Biol 50:115–132
11. Maini PK, Burke MA, Murray JD (1991) On the quasi-steady state assumption applied to Michaelis–Menten and suicide substrate reactions with diffusion. Phil Trans Roy Soc Lond A 337:299–306
12. Zhou H-X (1997) Theory and simulation of the influence of diffusion in enzyme-catalysed reactions. J Phys Chem B 101:6642–6651
13. Merkin JH, Sleeman BD (2005) On the spread of morphogens. J Math Biol 51:1–17
14. Morton KW, Mayers DF (2005) Numerical solution of partial differential equations. Cambridge University Press, Cambridge
15. Polyanin AD (2002) Handbook of linear partial differential equations for engineers and scientists. Chapman & Hall, New York
16. Pao CV (1992) Nonlinear parabolic and elliptic equations. Plenum Press, New York